International Journal of Applied Earth Observation and Geoinformation 35 (2015) 161–174

Contents lists available at ScienceDirect

International Journal of Applied Earth Observation and Geoinformation

journal homepage: www.elsevier.com/locate/jag

Drivers of land cover and land use changes in St. Louis metropolitan area over the past 40 years characterized by remote sensing and census population data

Maitiniyazi Maimaitijiang[a,c], Abduwasit Ghulam[a,*], J.S. Onésimo Sandoval[b], Matthew Maimaitiyiming[a]

[a] Center for Sustainability, Saint Louis University, St. Louis, MO 63108, USA
[b] Department of Sociology and Anthropology, Saint Louis University, St. Louis, MO 63108, USA
[c] College of Management, Xinjiang Agricultural University, Urumqi, Xinjiang 830052, China

ARTICLE INFO

Article history:
Received 3 April 2014
Accepted 26 August 2014

Keywords:
Urban growth
Land cover and land use
Geographically weighted regression

ABSTRACT

In this study, we explored the spatial and temporal patterns of land cover and land use (LCLU) and population change dynamics in the St. Louis Metropolitan Statistical Area. The goal of this paper was to quantify the drivers of LCLU using long-term Landsat data from 1972 to 2010. First, we produced LCLU maps by using Landsat images from 1972, 1982, 1990, 2000, and 2010. Next, tract level population data of 1970, 1980, 1990, 2000, and 2010 were converted to 1-km square grid cells. Then, the LCLU maps were integrated with basic grid cell data to represent the proportion of each land cover category within a grid cell area. Finally, the proportional land cover maps and population census data were combined to investigate the relationship between land cover and population change based on grid cells using Pearson's correlation coefficient, ordinary least square (OLS), and local level geographically weighted regression (GWR). Land cover changes in terms of the percentage of area affected and rates of change were compared with population census data with a focus on the analysis of the spatial-temporal dynamics of urban growth patterns. The correlation coefficients of land cover categories and population changes were calculated for two decadal intervals between 1970 and 2010. Our results showed a causal relationship between LCLU changes and population dynamics over the last 40 years. Urban sprawl was positively correlated with population change. However, the relationship was not linear over space and time. Spatial heterogeneity and variations in the relationship demonstrate that urban sprawl was positively correlated with population changes in suburban area and negatively correlated in urban core and inner suburban area of the St. Louis Metropolitan Statistical Area. These results suggest that the imagery reflects processes of urban growth, inner-city decline, population migration, and social spatial inequality. The implications provide guidance for sustainable urban planning and development. We also demonstrate that grid cells allow robust synthesis of remote sensing and socioeconomic data to advance our knowledge of urban growth dynamics from both spatial and temporal scales and its association with population change.

Introduction

With the growth of urbanization around the world, today, more than half of the world's population lives in urban regions, and this trend is projected to continue in the future decades (United Nations, 2014). Land cover and land use change (LCLUC) with urban growth is a global issue with paramount socioeconomic and environmental implications (Bhatta et al., 2010; De Freitas et al., 2013; Lopez et al., 2001; Xian and Crane, 2005). For example, LCLUC leads to a number of environmental problems including water quality degradation, air pollution, loss of biodiversity, urban heat island effects, social-economic disparities, social fragmentation, and infrastructure costs (Arnfield, 2003; Kalnay and Cai, 2003; Squires et al., 2002; Xian and Crane, 2005, 2006).

Post-industrial US cities have been experiencing urban sprawl growth spreading out over rural land at the periphery of urban area, while the population in the urban core is shrinking (Frumkin, 2002; Hasse and Lathrop, 2003). The St. Louis Metropolitan Statistical Area (STL) is an excellent example of urban sprawl where poverty, crime, and racial segregation are concentrated in inner city, while wealth

* Corresponding author. Tel.: +1 314 977 5156.
E-mail address: awulamu@slu.edu (A. Ghulam).

http://dx.doi.org/10.1016/j.jag.2014.08.020
0303-2434/

and environmentally rich resources are located in the suburban areas. The St. Louis City once was an industrial powerhouse of the Midwestern US with the 4th largest population in the nation in 1904. It has been undergoing urban sprawl with a shrinking urban core over the last several decades (Gordon, 2008).

Remote sensing, spatial statistics, and geo-informatics provide powerful tools to study urban environments (Griffiths et al., 2010; Sutton, 2003; Yang et al., 2003), urban growth modeling (Herold et al., 2003; Jat et al., 2008; Poelmans and Van Rompaey, 2009), and projecting socio-economical, environmental, and ecological effects of urban development (Gillies et al., 2003; Squires et al., 2002; Tu, 2013; Xian and Crane, 2006). Urban growth is a synthetic process, which includes not only biophysical change but also socioeconomic change (Lambin et al., 2003; Martinuzzi et al., 2007; Radeloff et al., 2000). Socioeconomic aspects are critical to further understand urban growth process and temporal and spatial patterns (Bagan and Yamagata, 2012; Banzhaf et al., 2013; De Freitas et al., 2013). Numerous studies have examined the relationship between LCLUC and socioeconomic data over the last two decades. Most of these studies were limited to regional scale socioeconomic data summarized for the metropolitan statistical area, city, or county level (Alperovich and Deutsch, 1992; Berry, 1990; Fox, 2003; Ma et al., 2008), which was unable to reveal the detailed spatial characteristics of LCLUC and socioeconomic factors. As these datasets became publicly available in recent years, census tract scale was also explored (De Freitas et al., 2013; Lo and Yang, 2002; Ryznar and Wagner, 2001; Xiao et al., 2006). However, many census tracts boundaries were not stable from the time period of study (Gallego, 2010; Martin, 1996; Small et al., 2011) and may not be suited for temporal statistical (Verburg et al., 2008). Most of these previous studies utilized global level statistical tools such as Pearson's correlation coefficient or Ordinary Least Square (OLS) to illustrate the relationship between LCLUC and socioeconomic data (Bagan and Yamagata, 2012; Lo and Yang, 2002). In fact, these statistical methods are based on two basic assumptions: (1) model residuals are uncorrelated with each other (no spatial autocorrelation) and (2) there is constant variance (homoscedasticity) (Fotheringham et al., 2003; Hamilton and Press, 1992). However, natural, social, and anthropogenic characteristics are not constant over space (Fortin, 1999; Tu, 2013), and some magnitude of spatial autocorrelation often are present in these data (De Freitas et al., 2013). Spatial autocorrelation has several implications for statistical inference testing (Fortin and Dale, 2009). For example, the presence of spatial autocorrelation in one or both variables may violate the assumption of independence among samples and thereby inflate the degrees of freedom in the traditional test of significance of a Pearson's correlation coefficient (Fortin and Payette, 2002). The efficiency of OLS would be reduced and the interpreted results would be misleading because of the existence of spatial autocorrelation (Bellehumeur and Legendre, 1998). In addition, global level statistics lack the ability to reveal and the varying relationships over space (Tu and Xia, 2008). For these reasons, geographically weighted regression (GWR), which is capable of capturing the spatial heterogeneity and variations in the relationships and account for spatial autocorrelation, has been suggested (Fotheringham et al., 2003).

The goal of this study was to identify the drivers of LCLUC in the STL region over the last 40 years by integrating remote sensing derived land use data with socioeconomic data. LCLU and census tract data were converted to 1-km grid cells. Global level and local level statistical approaches were employed to reveal the past and present patterns and processes and trends of urban growth. This paper contributes to our knowledge of urban developments in post-industrial US cities with comparative analysis of the role of various statistical tools on LCLUC studies. Other climate and environmental factors such as temperature and precipitation changes may influence LCLUC, but these factors were outside of the scope of this contribution. Climate change and its impacts on land use dynamics were discussed in recent publications (Jordan et al., 2012, 2014).

Study area and data

Study area

The St. Louis Metropolitan Statistical area is located at the junction of Missouri and Illinois and at the intersection area of the Missouri and Mississippi Rivers. In this study, we chose the East-West gateway region as our study area, which includes St. Louis City, St. Louis County, St. Charles County, Franklin County and Jefferson County for the Missouri part of the region and Madison County, St. Clair County and Monroe County for the Illinois part of the region (Fig. 1). The total area of this region is approximately 11,892 km^2, and much of the area is a fertile and gently rolling prairie that features low hills and broad, shallow valleys. The elevation of surface topography ranges from 68 m at Chester to 530 m at the hilly area of the south-west St. Louis County. It includes a diversity of land cover classes in the area such as forest, agriculture, and pasture and urban (Jordan et al., 2012). The climate of this region is continental type with distinct alteration of seasons characterized by wide ranges in temperature, and irregular annual and seasonal precipitation (NWS, 2014).

Data

Land use data

The Landsat program is significant in studying the earth's surface and associated change process (Cohen and Goward, 2004). We collected 17 Landsat MSS and TM images to generate LCLU maps for the study area from five separate dates (four MSS images for 1972 and 1982 respectively, three TM images for 1990, 2000, and 2010, respectively). Table 1 provides the detailed information about the images. These images were selected from relatively cloud-free acquisitions (<10%) and during the growing season. In addition, the time series of Landsat data were selected corresponding to the decadal census data (Banzhaf et al., 2013).

All Landsat images were geometrically rectified using ground control points (GCPs) from high resolution images to a common map reference system (UTM map projection Zoon 15 North, GCS_North_American_1983 Datum). The GCPs were dispersed throughout each scene and the registration accuracy was less than 0.5 pixels. Radiometric "bad" pixels on 1972 Landsat MSS images were identified visually and removed by on screen digitizing. Atmospheric correction was carried out using Quick Atmospheric Correction (QUAC) available with ENVI® image processing and analysis software from EXELIS Visual Information Solutions. The goal of atmospheric correction was to adjust the multi-temporal dataset to a common radiometric scale (Song et al., 2001).

Aerial photos, National Land Cover Dataset (NLCD) of 1992 and 2001 from United States Geological Survey, St. Louis Metropolitan Statistical Area LCLU data for 2010 ("Current Vegetation 2010") from Missouri Resource Assessment Partnership (MoRAP) and East-West Gateway Council of Governments were used to collect training samples and validate classification results.

Socioeconomic data

Socioeconomic data (i.e., population, race, and housing units) were obtained from US Census Bureau, Social Explorer Demographic Data center, and LTDB (Longitudinal Tract Data Base) of the US2010 project (http://www.s4.brown.edu/us2010/Researcher/Bridging.htm). US Census TIGER Products and National Historical Geographical Information System (NHGIS) shapefiles were joined with socioeconomic data.

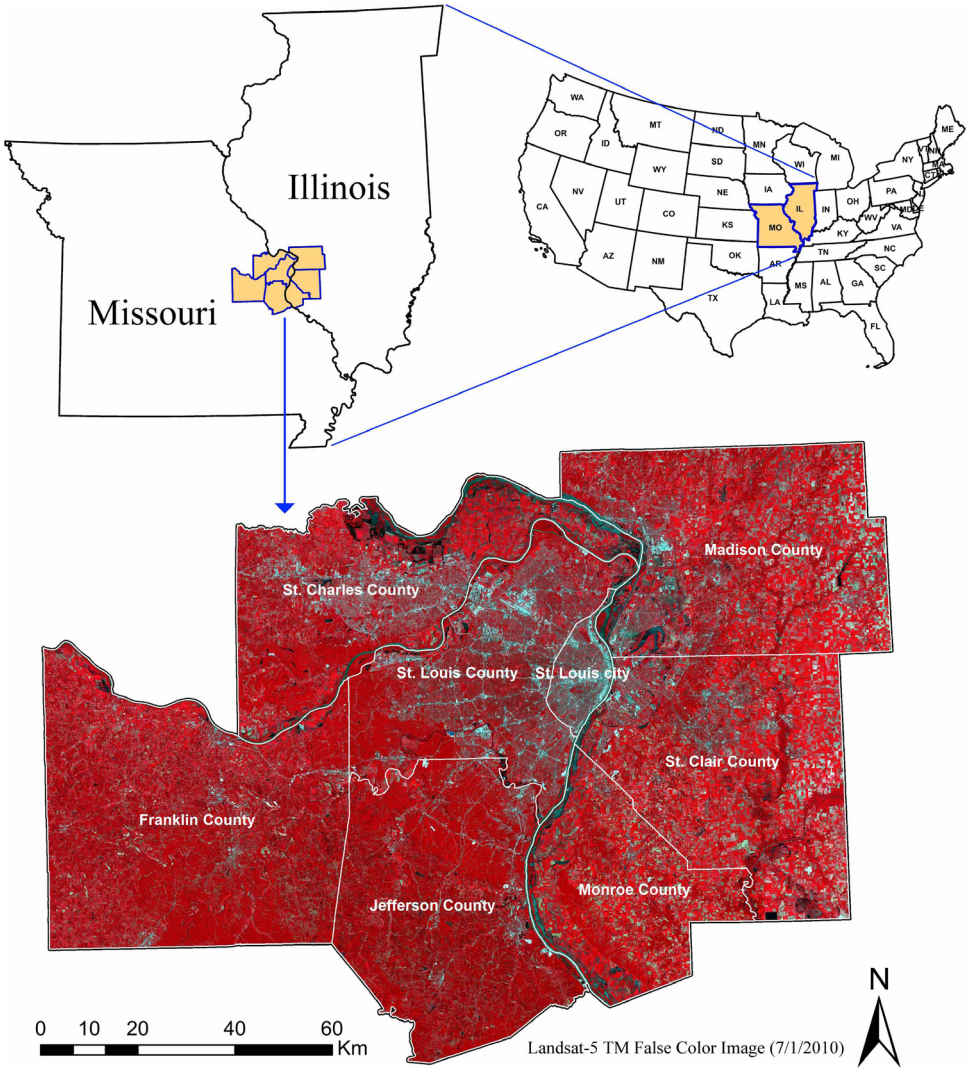

Fig. 1. Location of study area.

Methods

Land cover and land use classification

The National Land Cover Database (NLCD) is the most popular land cover data product widely used in the US. NLCD 2001 and 2006 share a similar classification scheme, but the 1992 and 2001 NLCD were based on different classification schema and models, severely limiting their comparability over time. The land cover change product derived from the NLCD 1992 and 2001 layers requires "retrofitting" to cross-reference the classifications (MRLC, 2008). However, monitoring LCLUC over time requires consistency among maps, both ontologically and statistically. Using NLCD to detect land cover change would lead to unreliable conclusions (Sexton et al., 2013). In addition, buildup areas such as roads and separate houses in agricultural lands were classified as agricultural land in the 1992 NLCD. However, our definition of buildup areas includes any human made land use which include roads. For these reasons, NLCD data cannot be used for temporal analysis with census data. Therefore, we applied a robust Support Vector Machine (SVM) classifier which is based on statistical learning theory (Cortes and Vapnik, 1995) for land cover classification consistently over time.

SVM employs a kernel function to map a set of non-linear decision boundaries in the original dataset into linear boundaries of a higher-dimensional construct (Han et al., 2007). SVM often outperforms other classifiers (Foody and Mathur, 2006; Huang and Wang, 2006; Kolios and Stylios, 2013), especially since it has been proven to be generally capable of analyzing high dimensional datasets and performs well even when training data is limited (Huang et al., 2002; Mantero et al., 2005).

Land cover is the biophysical cover on the earth's surface (e.g., water, vegetation, human made materials such as asphalt), and land use refers to the actions of people in a land cover to produce, change or maintain it (e. g., agriculture, commerce, settlement) (Jensen, 2009). Classification is using specific criteria (classifiers) to order or arrange objects (land cover) into groups or sets on the basis of their relationships (Sokal, 1974). In this paper, we applied Anderson Land Cover Classification System (Anderson, 1976). An initial unsupervised classification using ISODATA algorithm revealed that water was spectrally distinct from the land classes, but forests class was confused with shrub and swamps (predominantly deciduous) due to their spectral similarity on Landsat images. Various types of forest including deciduous forest, mixed forest, shrubs, and swamps were set as forest class. At 30 m Landsat spatial resolution, grass and cropland was not spectrally discriminated as well. Any type of impervious surface including buildings, roads, and concrete pavements were all identified as buildup areas. Buildup area was spectrally unique but confused with barren land. On high resolution ancillary data and field investigation, we found that the proportion of barren land was actually very small in this area and

Table 1
Landsat images used in this study.

Year	Sensor	Date(m/d/y)	Path/Row	Spatial resolution(m)
1972	Landsat-1 MSS	10/2/1972	25/33	79
	Landsat-1 MSS	10/2/1972	25/34	
	Landsat-1 MSS	8/28/1972	26/33	
	Landsat-1 MSS	8/28/1972	26/34	
1982	Landsat-4 MSS	9/30/1982	24/33	79
	Landsat-4 MSS	9/30/1982	24/34	
	Landsat-4 MSS	10/25/1982	23/33	
	Landsat-4 MSS	10/25/1982	23/34	
1990	Landsat-5 TM	8/27/1990	24/33	30
	Landsat-5 TM	10/14/1990	24/34	
	Landsat-5 TM	9/5/1990	23/33	
2000	Landsat-5 TM	9/7/2000	24/33	30
	Landsat-5 TM	9/7/2000	24/34	
	Landsat-5 TM	8/31/2000	23/33	
2010	Landsat-5 TM	7/1/2010	24/33	30
	Landsat-5 TM	7/1/2010	24/34	
	Landsat-5 TM	6/24/2010	23/33	

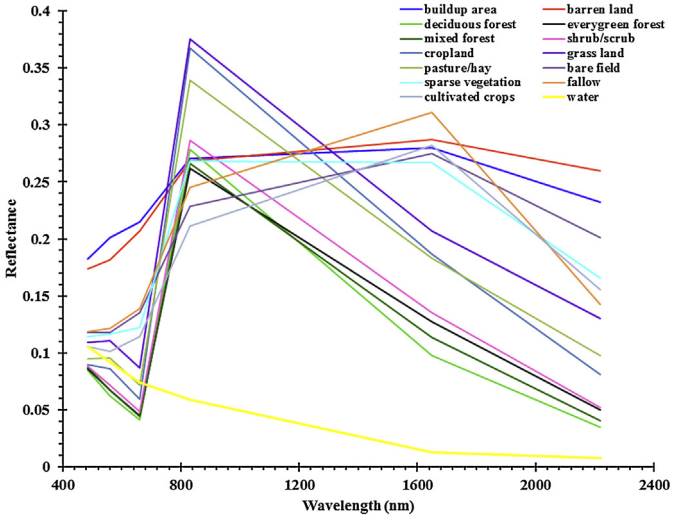

Fig. 2. Spectral profiles of different land cover types from Landsat TM (8/31/2000).

consisting of strip mines or quarries with building constructions. Therefore, barren land was merged into buildup area. There were great similarity among pasture/hay, and grass land within urban area such as green parks, golf courses, and green open space, we defined these land covers as one type. Cultivated crops (such as corn, soybeans, vegetables, tobacco, and cotton), bare fields, sparse vegetation and fallow demonstrate relatively unique spectral characteristics.

Uncertainties in classification results are unavoidable. Misclassification usually happens due to spectral confusion and reflectance similarity among land cover types such as barren land with high-density urban, urban grass/lawn cover with cropland (Lu and Weng, 2006; Sexton et al., 2013; Yuan et al., 2005). To the degree possible, classes should be defined such that they are distinct at the temporal and spatial grain of analysis, clearly identifiable in reference datasets, and based on discrete types in reality (Kelly et al., 1999). Hierarchical and generalized schemas can help to trap errors between specific classes within genera or broader levels of association and yield high accuracy (Sexton et al., 2013). Considering the above mentioned uncertainties in classification caused by spectral confusion and reflectance similarity (Fig. 2), we combined these "spectrally similar" land cover types, our final classification system was generalized into four land cover and land use classes: buildup, field, forest, and water for time series comparison (Table 2).

Training samples were obtained using polygon vectors and raster points designed for each land cover type. These samples were photo interpreted from Landsat images, high-resolution aerial photos, USGS NLCD maps, and verified by our expert knowledge of the study area. We randomly collected 2000–8000 training samples (pixels) for per land cover class, respectively. We collected additional samples for validation and accuracy assessment. In addition, we applied post-classification refinements for the results to reduce classification errors caused by the similarities in spectral responses of certain classes, especially for bare fields and buildup land.

It should be noted that to minimize the classification inaccuracy due to the color differences among different images of the single time-frame considered (several images cover the study area), we applied classification for each image separately, then mosaicked them to form a whole area land cover map. This was also helpful in eliminating atmospheric dissimilarities on the days the images were acquired.

Classification accuracy assessment

We used producer's accuracy (PA), user's accuracy (UA), overall accuracy (OA), and the Kappa statistic coefficient (Kappa) as validation metrics based on selected independent testing samples to evaluate the performance of SVM classifier. In addition, to assess how well the Landsat classifications performs compared to other land cover inventories, the results of Landsat classifications for 1990 and 2000 were compared to the National Land Cover Dataset (NLCD) for 1992 and 2001 respectively, and the result of 2010 was compared to the 6 m LCLU map provided by the Missouri Resource Assessment Partnership (MoRAP).

Grid cell approach

We created blank vector polygon with kilometer square grid cells using the Risk Terrain Modeling (RTM) tool, which was downloaded freely from Rutgers Center on Public Security. We assigned the time-period LCLU and socioeconomic census data to the empty grid cells by spatial join function of ArcGIS from ESRI. In the

Table 2
Land cover classification scheme.

Generalized land cover classes	Description	
Buildup land	All residential, commercial and industrial area, transportation infrastructure, settlements	
Water	Permanent open water, lakes, reservoirs, streams, bays and estuaries	
Forest	Deciduous forest land, evergreen forest land, mixed forest land, dwarf scrub and shrub/scrub land, woody wetlands	
Field	Cultivated and fallow	Cultivated crops such as corn, soybeans, vegetables, tobacco, and cotton; Bare fields, sparse vegetation
	Grass and cropland	Urban/Recreational Grasses including green parks, golf courses, lawns, and sod fields; croplands; pasture/hay.

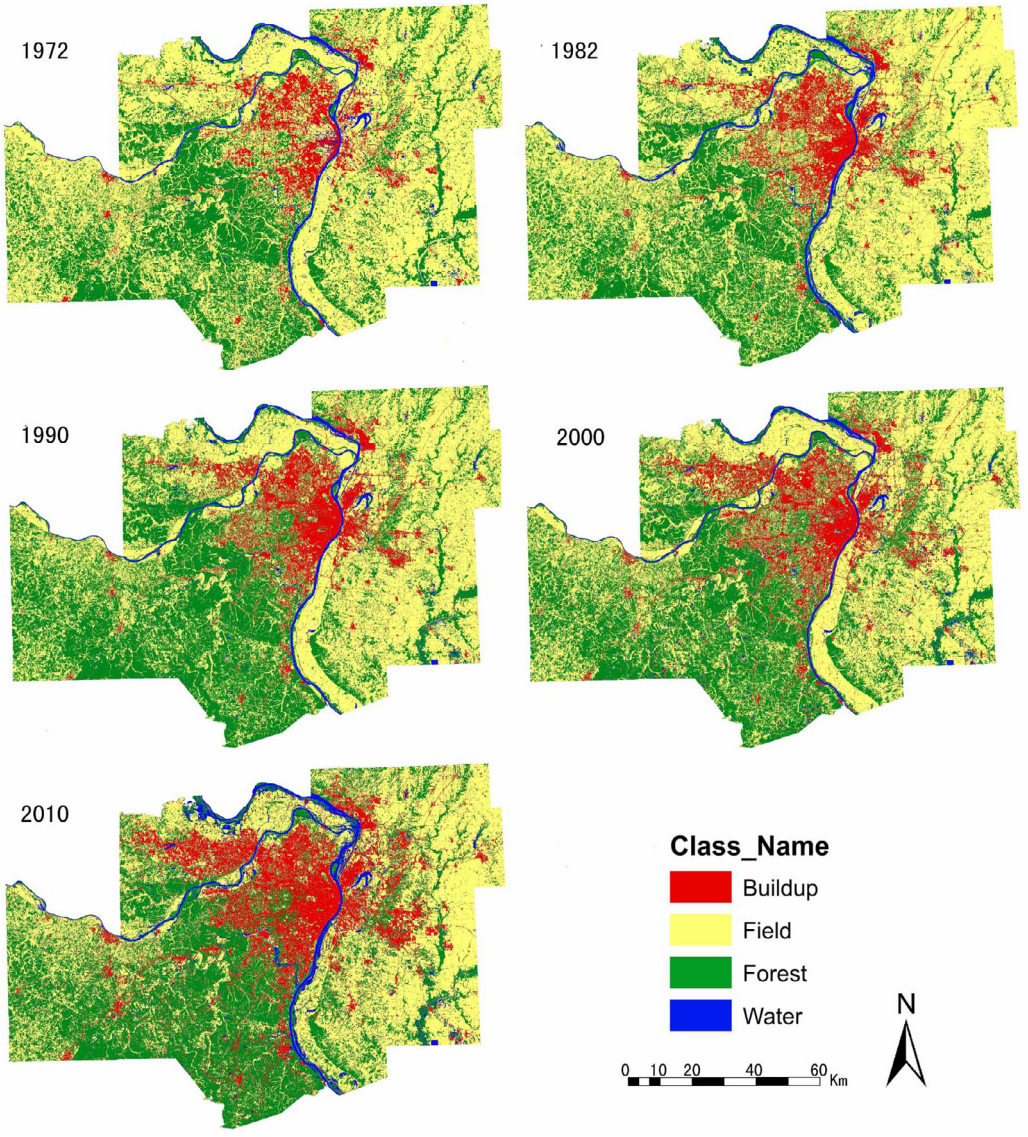

Fig. 3. Land cover and land use maps of study area for 1972, 1982, 1990, 2000, and 2010.

following two paragraphs, we will describe the procedures of converting LCLU and socioeconomic data into grid cells.

Grid cell LCLU data

To quantify the percent area and percentage of change of land cover types within a 1-km grid cell, the LCLU data were apportioned to the grid cells. To calculate the percentage of a land cover type within a cell, the sum of the land cover type area of all pixels that overlaid with the cell was divided by the area of the cell. Converting the data into grid cells, however, was not straightforward at the boundary where different land cover types intersect with the grid cell. One approach was to assign the pixel located on a grid line (or spanning multiple grid lines) to the cell that covered the largest part of the pixel (Bagan and Yamagata, 2012). However, this may introduce some errors to grid cell statistics. For example, it is possible that the sum of all land cover areas obtained from the pixels overlapped with the cell can be larger than the area of the grid cell itself. To overcome this limitation, we converted each raster LCLU map to vector grids, and then it was intersected with 1-km empty grid cell. This process divided the land cover patch in LCLU vector map into pieces so that data fit into the 1-km grid cells by its proportion. Then, the sum of the area of each patch piece (A_t) within the grid cell was divided by the 1-km cell area to calculate the percentage (P_t) of each land cover type.

$$P_t = \frac{\sum_{i=0}^{n} A_t}{A_g} \times 100\% \quad (1)$$

P_t is the percentage of land cover type t in one grid cell. A_t is area of each piece of land cover type t in one grid cell. n is the number of the pieces of land cover type t in one grid cell. A_g is the area of each grid cell, in this case it is 1 square kilometer.

Grid cell census data

Census tract level socioeconomic data tables from Social Explorer Demographic Data center (www.socialexplorer.com) were joined to US Census TIGER shapefiles using Arcgis10.1 software. The main variables used include population, race and ethnicity, house units, and vacant house units. Then we converted these census tract scale socioeconomic data to 1-km scale grid cell maps using the following steps.

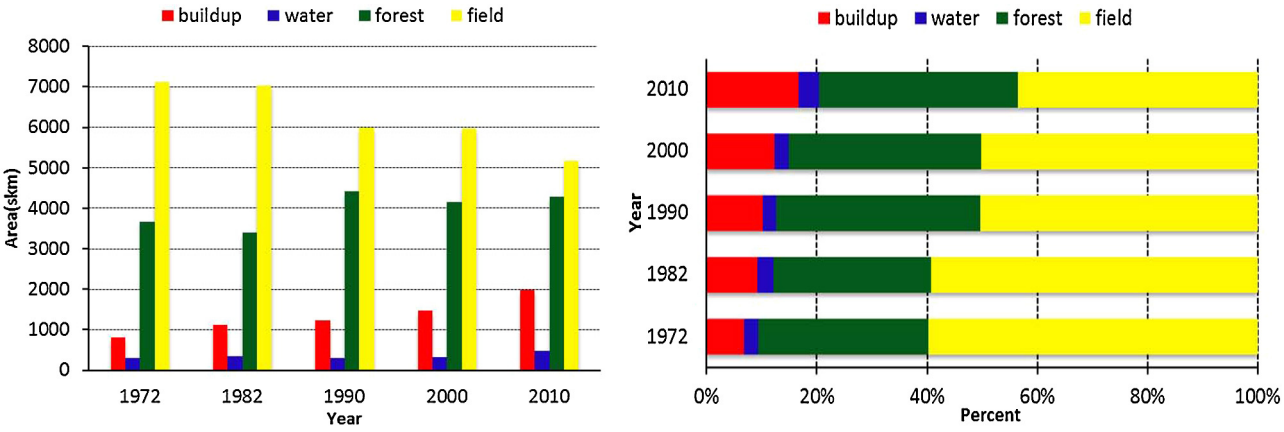

Fig. 4. Total area and percentages of each land cover category between 1972 and 2010.

First, dividing variables such as population number, house units in each census tract by the corresponding census tract's area, we estimated the density of each variable at each census tract scale (D_v) and added it as a new variable in the attribute table. Then, we intersected this census tract scale socioeconomic data with 1-km grid cell shapefile. This process divided each census tract into pieces that fit into the grid cells, and the density of each variable in each pieces remained the same. The area of each piece within one grid cell (A_v) was multiplied by the density of the variable (D_v) being gridded. Finally, sum of these values for all tract pieces were aggregated in the grid cell by the follow equation:

$$C_v = D_v \times \sum_{i=1}^{n} A_v \tag{2}$$

C_v is the total count of variable v in each grid cell, v is variable type such as population, house units. D_v is density of variable v. n is the total number of census tract pieces of variable v in one grid cell. A_v is the area of each tract piece of variable v in one grid.

Converting LCLU maps and socioeconomic data to grid cells enabled us to aggregate each input variables and to calculate their proportions in basic grid cells. Furthermore, this allowed us to effectively evaluate the spatial-temporal changes in LCLU and population, exploring the patterns of urban sprawl over the last 40 years using the statistical approach detailed below.

Statistical methods

We began the analysis by using the Pearson's correlation coefficient and Ordinary Least Regression (OLS) to reveal the relationship between LCLU and population change at global scale. Then, we used Geographically Weighted Regression (GWR) analysis to explore the local spatial relationship among the variables. The GWR method was originated from the OLS and smoothing techniques. It has been developed to explore spatially varying relationships and to account for spatial autocorrelation. The output is a series of location-specific parameters that visualize geographical interactions. It also produces a global R^2 to show the overall performance of the GWR model (Fotheringham et al., 2003). In addition, we employed the Global Moran's I statistic to identify the existence and intensity of spatial autocorrelation of variables (Harries, 2006). The Global Moran's I examined the spatial autocorrelation in models residuals of OLS and GWR to assess and compare their ability to reduce spatial autocorrelation (Su et al., 2012; Zhang and Gove, 2005). The value of Moran' I varies from −1 to 1. The values −1, 0, and 1 indicate negative spatial autocorrelation, randomness, and positive spatial autocorrelation, respectively (Moran, 1950).

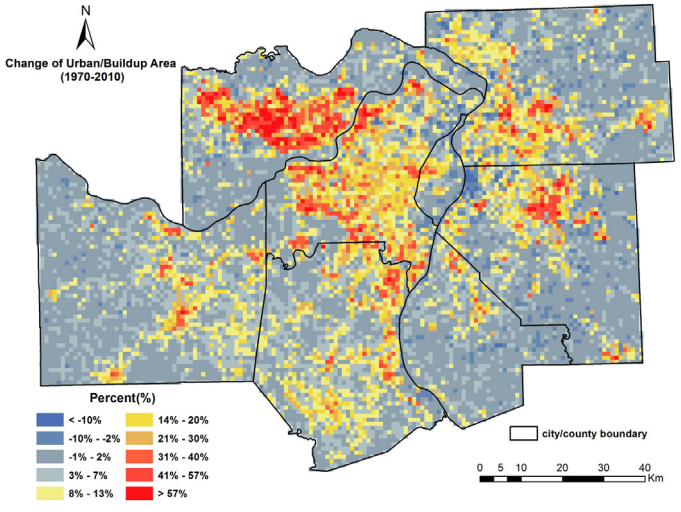

Fig. 5. Percentage change of buildup area from 1972 to 2010.

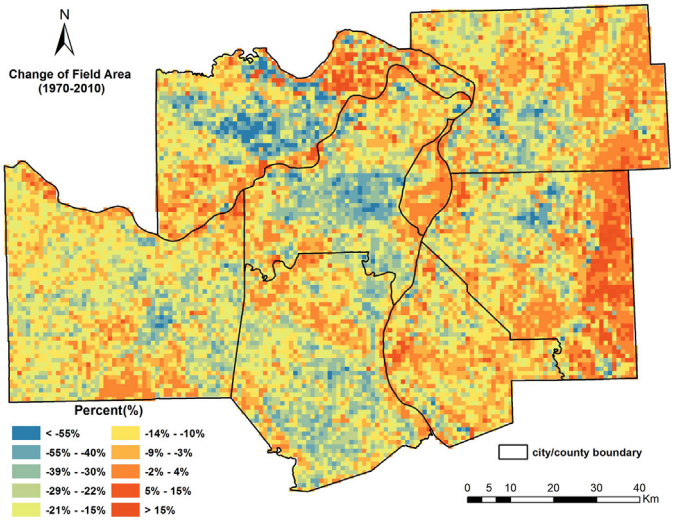

Fig. 6. Percentage change of field area from 1972 to 2010.

Table 3
Accuracy assessment of classification results based on confusion matrix for 1972, 1982, 1990, 2000 and 2010.

	Buildup	Forest	Water	Fallow	Agriculture	Total	UA (%)
1972							
Buildup	3018	0	6	281	64	3369	89.58
Forest	0	8457	13	6	134	8610	98.22
Water	1	1	3445	34	197	3678	93.67
Fallow	58	0	21	2185	339	2603	83.94
Agriculture	12	63	33	142	1712	1962	87.26
Total	3089	8521	3518	2648	2446	20,222	
PA (%)	97.70	99.25	97.92	82.52	69.99		
OA (%)	93.05						
Kappa	0.91						
1982							
Buildup	2985	0	0	0	4	2989	99.87
Forest	0	8683	4	0	22	8709	99.70
Water	3	0	3041	0	6	3050	99.70
Fallow	132	0	0	3634	0	3766	96.49
Agriculture	12	2	0	0	2567	2581	96.49
Total	3132	8685	3045	3634	2599	21,095	
PA (%)	95.31	99.98	99.87	100.00	98.77		
OA (%)	99.12						
Kappa	0.98						
1990							
Buildup	2780	0	0	61	8	2849	97.58
Forest	0	7960	6	0	88	8054	98.83
Water	0	7	2516	0	0	2523	99.72
Fallow	200	1	0	3580	3	3784	94.61
Agriculture	7	89	0	5	3110	3211	96.85
Total	2987	8057	2522	3646	3209	20,421	
PA (%)	93.07	98.80	99.76	98.19	96.91		
OA (%)	97.67						
Kappa	0.97						
2000							
Buildup	2717	0	0	30	0	2747	98.91
Forest	1	8269	8	0	17	8295	99.69
Water	1	1	2441	0	10	2453	99.51
Fallow	42	0	1	2915	10	2968	98.21
Agriculture	8	16	16	19	3315	3374	98.25
Total	2769	8286	2466	2964	3352	19,837	
PA (%)	98.12	99.79	98.99	98.35	98.90		
OA (%)	99.09						
Kappa	0.98						
2010							
Buildup	2600	0	0	93	1	2694	96.51
Forest	3	8132	0	0	97	8232	98.79
Water	8	1	2538	0	0	2547	99.65
Fallow	124	0	0	2828	0	2952	95.80
Agriculture	10	102	0	0	2801	2913	96.16
Total	2745	8235	2538	2921	2899	19,338	
PA (%)	94.72	98.75	100.00	96.82	96.62		
OA (%)	97.73						
Kappa	0.97						

PA, producer's accuracy; UA, user's accuracy; OA, overall accuracy; Kappa, kappa coefficient.

Results

Land cover and land use change

Land cover and land use maps for 1972, 1982, 1990, 2000, and 2010 are presented in Fig. 3. Fig. 4 shows the area of each land cover category and its percentage in the total area. It is apparent that buildup areas increased from 812 km^2 (6.8%) to 1980 km^2 (16.7%) from 1972 to 2010 (Fig. 4). The field and forest classes were the most dominant land cover in the region. Field areas exhibited a decreasing trend, dropping from 7108 km^2 to 5171 km^2 with its percentage from 59.8% to 43.5%. The forest land cover class increased over the last four decades from 30.8% in 1972 to its peak 37.1% in 1990, then it was maintained around 35.0% until 2010. This was consistent with a previous study (Manson and Evans, 2007) that there had been a significant level of reforestation in the Midwestern US in recent years. Despite a significant increase in population, the reforestation is occurring on former agricultural land and/or on formerly mined lands (Manson and Evans, 2007). Water body remained around 300 km^2 (2.5%) with a slight increase to 450 km^2 (3.9%) in 2010, which might be attributed to the seasonal variations of precipitation in the region.

In order to evaluate the spatial distribution of land cover changes, we created grid cell maps by overlying land cover maps on the empty grid cells and calculated the percentage of the land cover types within each cell. Fig. 5 shows the grid-cell based spatial changes of buildup areas from 1972 to 2010, which was calculated by subtracting the buildup area of 1972 from that of 2010 within the same gird, and then dividing the changed area by the cell area. As illustrated in Fig. 5, buildup areas increased in outer suburbs especially in St. Charles County, south part of St. Louis County and north-central part of St. Clair County. In contrast, a slight decrease

Table 4
Comparison of SVM classification results with NLCD and MoRAP datasets.

Year	Data resources	Each land class percentage of total study area			
		Buildup	Field	Forest	Water
1990	SVM	10.23%	50.24%	37.10%	2.43%
1992	NLCD	11.03%	52.96%	33.63%	2.38%
2000	SVM	13.28%	49.19%	34.80%	2.73%
2001	NLCD	14.58%	45.26%	37.53%	2.63%
2010	SVM	16.66%	43.49%	35.97	3.89%
2010	MoRAP	20.79%	43.64%	32.39%	3.18%

was observed in the urban core mainly occurring in St. Louis City, north part of St. Louis County and west part of St. Clair County. Fig. 6 shows the grid-cell based spatial changes of field areas from 1972 to 2010. A significant decrease took place in the area where the buildup area increased. A slight increase of field areas were found mainly in the St. Louis City, which was due to increased lawn and grass cover taken place on abandoned properties.

Land cover and land use change accuracy assessment

Accuracy assessment based on confusion matrices between classification maps and training samples showed an overall accuracy higher than 95% and kappa coefficient of 0.95 for 1982, 1990, 2000 and 2010, and 93% and 0.95 for 1972, respectively (Table 3). As a reference, we also compared classification maps of 1990, 2000, and 2010 with the 1992 and 2001 NLCD datasets and 2010 MoRAP data, respectively. As shown in Table 4, there were slight differences between them, but overall both datasets were consistent. The differences were due to the fact that our classification scheme was different than of the NLCD dataset. For example, build up areas (e.g., roads and houses) in agricultural fields were classified as farmland in NLCD data, but were build up areas in our classification systems. Build up areas in MoRAP includes grassland and open space within urban area but they were not classified that way in our scheme.

Population change

The overall population for the study area decreased by 2.7% from 2.38 million in 1970 to 2.32 million in 1982. The population consistently increased after the 1980s and reached 2.57 million in 2010. Comparing with the overall population of the study area, county/city level population change over the same time frames showed different trends (Fig. 7). For example, the population for

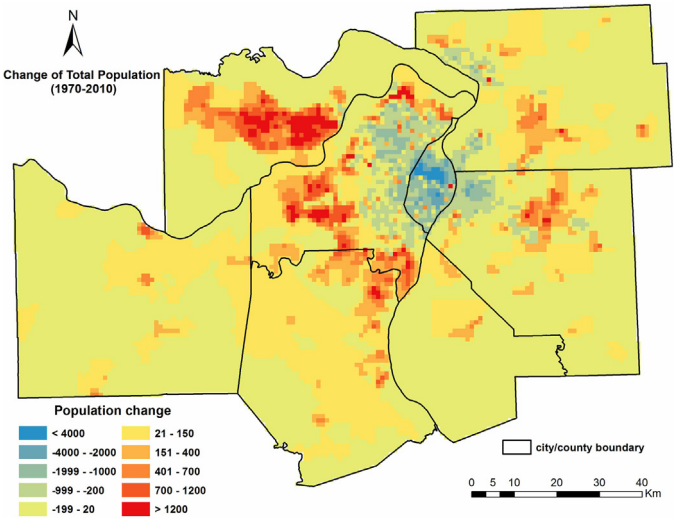

Fig. 8. Total population change from 1972 to 2010.

St. Charles County experienced continuous rapid growth characterized by 267.5% increase from 92,954 in 1970 to 360,485 in 2010, while population in St. Louis city declined continuously by 48.7% from 622,236 in 1970 to 319,240 in 2010. Other counties showed relatively slight growth in population size except for St. Clair County, which showed a slight decline over the time period.

The spatial distribution of population change within the grid cell is shown in Fig. 8. The population decreased in the central city and inner suburbs, and increased in outer suburbs especially in St. Charles County and south of St. Louis County. In general, this pattern was similar with the increase and decrease trends of white and black populations (Fig. 8). There was a significant decline in white population in St. Louis City and inner suburbs especially in north east part of St. Louis County and a significant increase in surrounding outer suburbs especially in St. Charles county and south of St. Louis county (Fig. 9) from 1970 to 2010. The spatial distribution of blacks exhibited different characteristics (Fig. 10), with the scope and scale of the distribution being smaller and mainly limited to the central region and inner suburbs. There was an obvious decrease in the black population in the north central part of St. Louis City and significant increase in south east part of the city. The north part of St. Louis County also experience decreased in the white population.

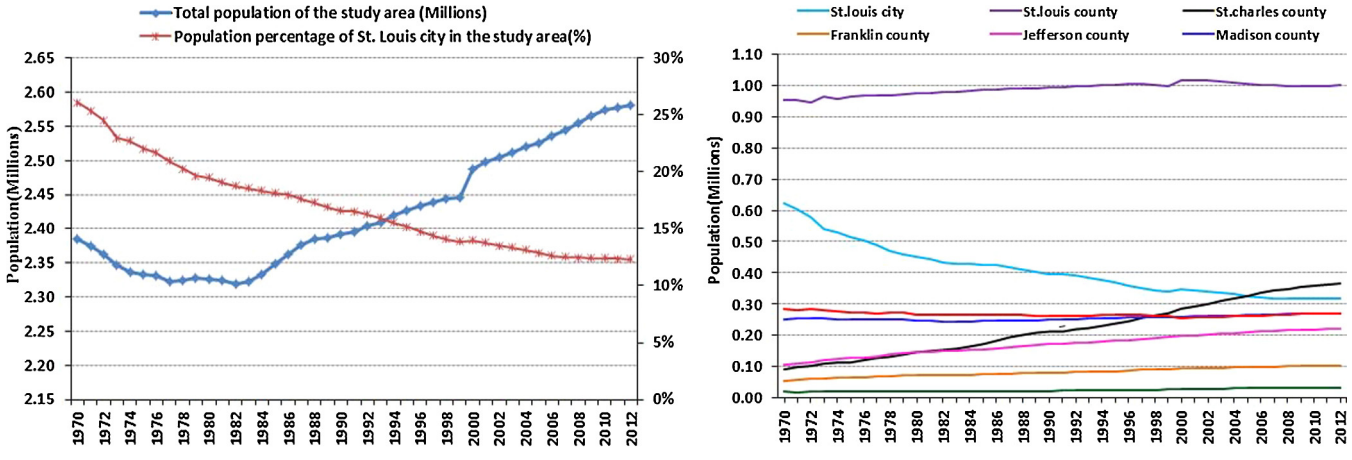

Fig. 7. Population change for the study area and county/city during 1970–2010.

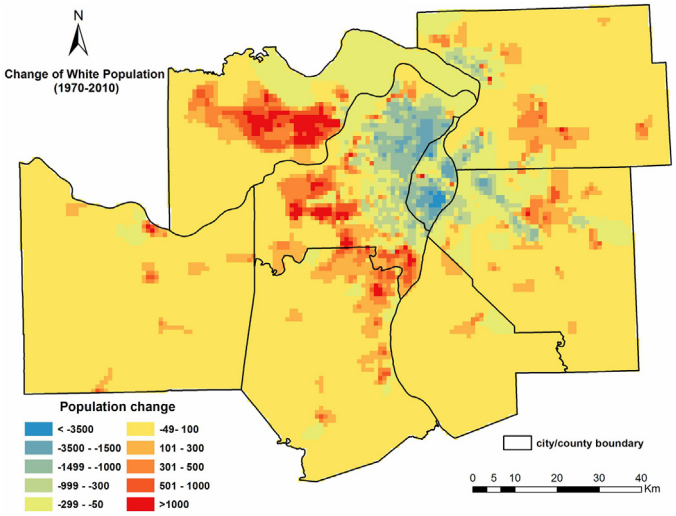

Fig. 9. White population change from 1972 to 2010.

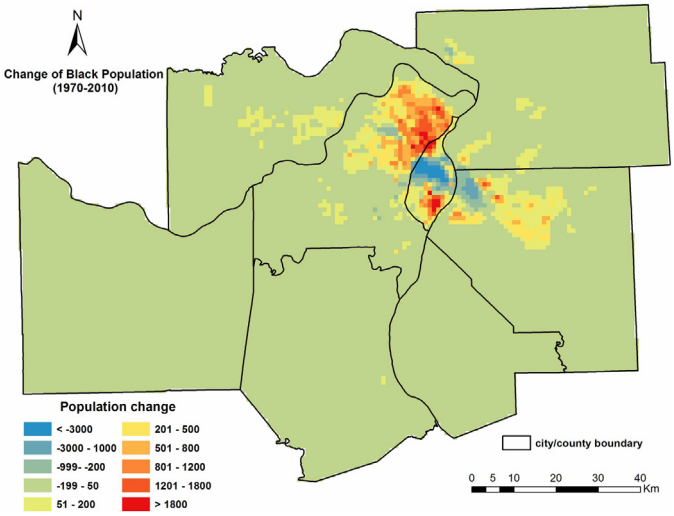

Fig. 10. Black population change from 1972 to 2010.

Relationship between land cover categories and population changes

Relationships based on Pearson's correlation coefficient

We investigated the relationship between the amount of each land cover category and population change using different statistical methods. First, we calculated Pearson's correlation coefficient (r) among the mentioned variables based on the grid cells. Table 5 presents a summary of coefficient matrices between changes of land cover categories and population changes (i.e., total population, white, and black) from 1970 to 2010. We used all 11,899 grid cells in the study area for the statistical analysis.

As shown in Table 5, the linear correlation coefficient was −0.659 between buildup and field, indicating increased buildup areas were developed on agricultural lands. Next, a stronger relationship was found between buildup and total population (r = 0.277), which was primarily explained by the changes in white population (r = 0.270). The correlation coefficient between the field and total population was −0.213, while forest change was negatively correlated with field (r = −0.564). The implication was that urban sprawl may have occurred in field, and at the same time, forest growth mostly gained acreage from field land cover. The correlations mentioned above were all statistically significant at $p < 0.01$ level.

To further understand the trends of urban growth, we divided the urban growth process into two time intervals, 1970–1990 and 1990–2010. The correlation analysis for the two time intervals is reported in Table 6. The correlation between the buildup and field relationship during these time frames were negative, −0.366 and −0.575, respectively. The correlation between the buildup and

Table 5
Pearson's correlation coefficient (r) between the changes of land cover categories during 1972–2010 and population change during 1970–2010.

r	Buildup	Field	Forest	Water	Population	White	Black
Buildup	1						
Field	−0.659**	1					
Forest	−0.165**	−0.564**	1				
Water	−0.032**	−0.221**	−0.100**	1			
Population	0.277**	−0.213**	−0.009	0.003	1		
White	0.270**	−0.206**	−0.014	0.009	0.712**	1	
Black	0.006	−0.014	0.014	−0.002	0.483**	−0.265**	1

** Correlation is significant at the 0.01 level (2-tailed).

Table 6
Pearson's correlation coefficient (r) between the changes of land-cover categories and population during the past 40 years (2 time intervals).

Period	r	Buildup	Field	Forest	Water	Population	White	Black
1970–1990	Buildup	1						
	Field	−0.366**	1					
	Forest	−0.260**	−0.779**	1				
	Water	−0.185**	−0.042**	−0.029**	1			
	Population	−0.232**	0.118**	−0.016	0.201**	1		
	White	−0.091**	0.042**	−0.013	0.119**	0.750**	1	
	Black	−0.241**	0.125**	0.000	0.139**	0.459**	−0.242**	1
1990–2010	Buildup	1						
	Field	−0.575**	1					
	Forest	−0.252**	−0.518**	1				
	Water	−0.085**	−0.065**	0.120**	1			
	Population	0.335**	−0.185**	−0.108**	−0.011	1		
	White	0.278**	−0.127**	−0.139**	0.005	0.652**	1	
	Black	0.027**	−0.043**	0.038**	−0.008	0.417**	−0.380**	1

** Correlation is significant at the 0.01 level (2-tailed).

Table 7
Moran's I for Buildup area and population change in different time intervals.

Variables	Moran' I		
	1970–2010	1970–1990	1990–2010
Buildup change	0.6437	0.6024	0.6101
Population change	0.8041	0.6992	0.5937

Statistical significant level: $p < 0.01$.

population relationship was negative for 1970–1990 ($r = -0.260$), but positive for 1990–2010 ($r = 0.335$). This was partly due to the decease and then increase of the total population during the two time intervals. Meanwhile, buildup were negatively correlated with the black population ($r = -0.241$) and showed a very poor correlation with white population during 1970–1990. In contrast, a positive correlation was found between buildup and the white population ($r = 0.278$) while there was no correlation with the black population during 1990 and 2010. The forest and field relationship had a strong negative correlation for both time intervals: −0.779 and −0.518, respectively. Water had almost no correlation with other variables. Correlation coefficient between the white and black population were −0.242 and −0.380 for the two time intervals, respectively.

Relationships based on OLS and GWR model

To further investigate the relationship between land cover categories and population changes, we applied OLS and local level spatial statistics using GWR. Our focus here was the spatial distribution of statistical relationship between the buildup and total population change, which were considered the most important variables that dictated the physical and socioeconomic aspects of urban sprawl.

The global Moran' I was calculated to illustrate the existence and intensity of spatial autocorrelation of the variables. Moran' I of each variable including buildup and population changes for all time intervals was higher than 0.6 (Table 7), which indicated that the variables were highly spatially clustered and auto-correlated.

OLS and GWR method were both carried out for the buildup and population relationship. We employed two statistical parameters to compare the model performance between GWR and OLS: adjusted squared correlation coefficient (R^2) and Akaike Information Criterion (AIC) (Akaike, 1974). R^2 measures goodness of fit, which varies from 0 to 1. When more variance is explained for the dependent variable, the R^2 tends to be higher. The stronger ability of the regression model to reflect reality is described by lower AIC values (Fotheringham et al., 2003). Better model performances are indicated by higher adjusted R^2 and lower AIC values. In addition, the statistical significance was also tested by an F-test. Table 8 shows that during 1970–2010, adjusted R^2 for the OLS model between the buildup and population relationship was 0.077, suggesting that population changes could explain only 7.7% of buildup changes. In comparison, R^2 of GWR model was 0.418, which indicates that population changes can explain 41.8% of buildup changes. Similar trends and improvements in R^2 with GWR over OLS were also found for the decadal intervals of 1970–1990 and 1990–2010. As can be seen from Table 8, the GWR model produced relatively lower AIC value compared to OLS, which indicated a better fit to the observed data and better model performance.

Table 9
Comparison of Moran' I of residuals from OLS and GWR models for different time intervals.

Model	Moran' I for residuals		
	1970–2010	1970–1990	1990–2010
OLS	0.5609	0.5772	0.5426
GWR	0.2168	0.1994	0.2117

OLS, ordinary least squares; GWR, geographically weighted regression; Statistical significant level: $p < 0.01$.

The spatial randomness of residuals was employed as the diagnostic measure of the regression model. A higher randomness indicates better model performance (Zhang and Gove, 2005). Moran' I for residuals from each of the OLS and GWR models were calculated (Table 9). Significant positive spatial autocorrelations were found for all OLS models, characterized by Moran's I ranging from 0.543 to 0.561 and $p < 0.01$, and all GWR models, characterized by Moran's I ranging from 0.199 to 0.217 and $p < 0.01$. The results showed that the GWR models produced much smaller global Moran's I than OLS models with the same independent variable, indicating that GWR models improved the reliability of the relationships by reducing the spatial autocorrelations in residuals, and GWR model was an improvement of the OLS model.

Spatial heterogeneity in relationships between buildup and population changes

The slope parameters (local regression coefficient) and local R^2 from GWR model for buildup and population changes are shown in Fig. 11. In contrast to the significant positive correlation between buildup and population change observed for 1970–2010 from Pearson's correlation coefficient (Table 5) and OLS model (Table 8), both significant positive and negative correlations were observed spatially by the GWR model (Fig. 11). Relatively strong positive relationships between buildup and population and higher R^2 were located in suburbs, specifically in St. Charles County, and the southwest part of St. Louis County, which experienced rapid buildup and population increase (Figs. 5 and 8). Negative relationships and high local R^2 values were found in St. Louis city. This finding is associated with the shrinking population and relatively stable (no development) buildup land in the city.

Spatial pattern of relationships between buildup and population changes were investigated for 1970–1990 (Fig. 12) and 1990–2010 (Fig. 13) time intervals. Comparing to Pearson's correlation coefficient (Table 5) and OLS model (Table 8) which showed only negative relationship between buildup and population changes during 1970–1990, Fig. 12 indicated that both significant positive

Table 8
Buildup area and population change regression analysis using different models for different time intervals.

Model	Parameters	Population change			
		1970–2010	1970–1990	1990–2010	
Global level	OLS	Adjusted R^2	0.077	0.032	0.112
		AIC	−18,488	−23,141	−21,272
		Coefficient	0.000082	−0.000055	0.000200
Local level	GWR	Adjusted R^2	0.418	0.495	0.530
		AIC	−23,795	−30,206	−28,147

$p < 0.01$; AIC, Akaike info criterion; OLS, ordinary least squares; GWR, geographically weighted regression.

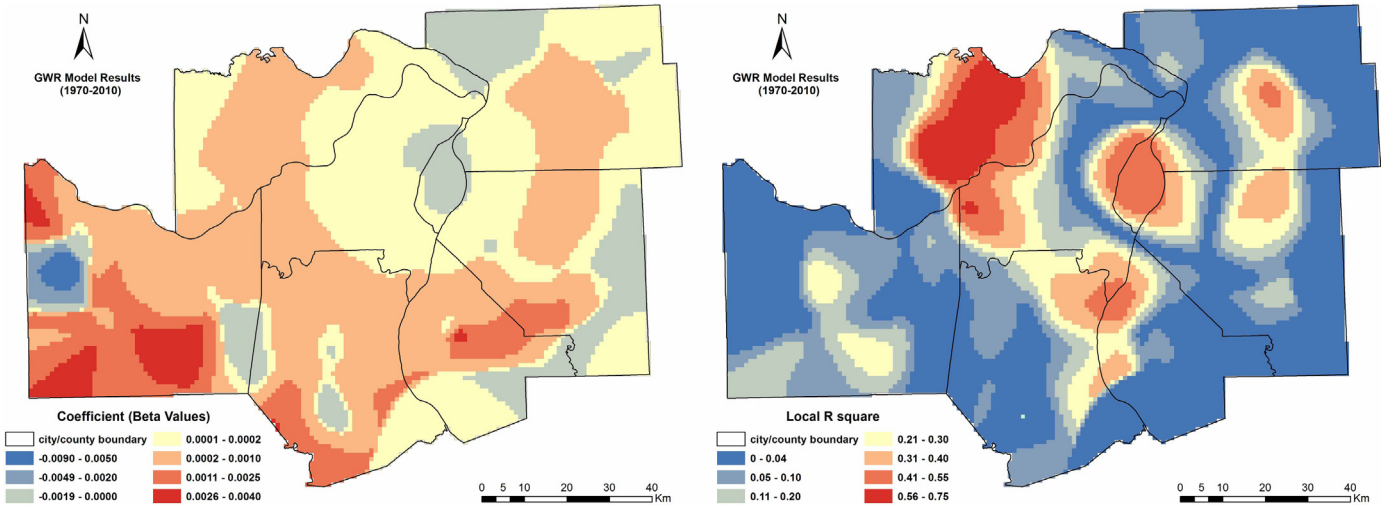

Fig. 11. Spatial variation of regression outputs from the GWR model for buildup area and population change during 1970–2010.

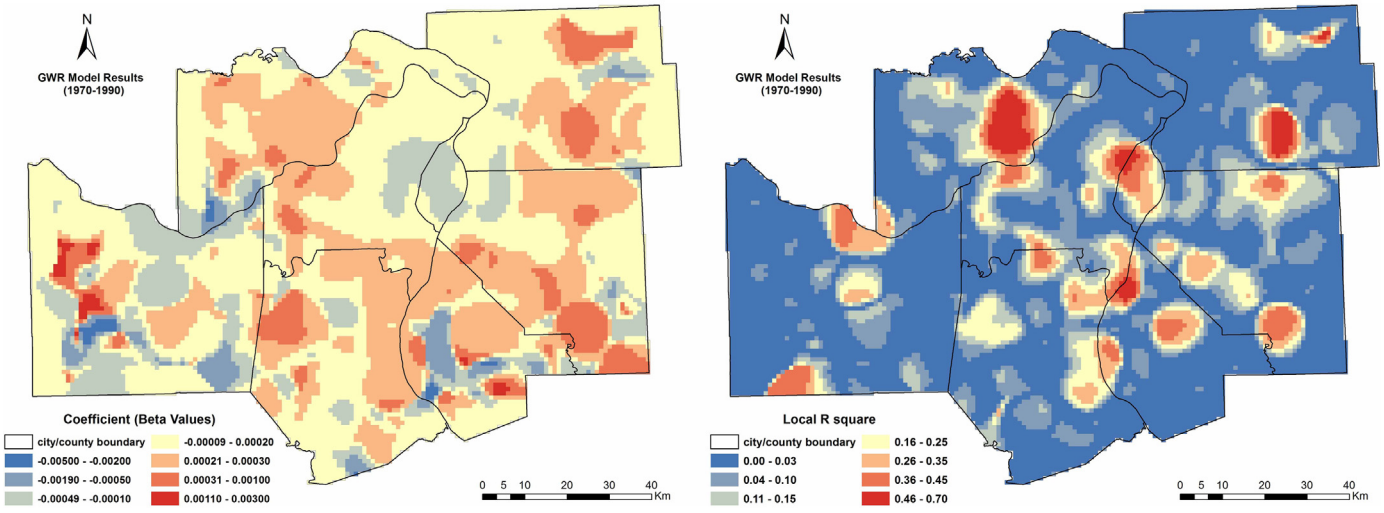

Fig. 12. Spatial variation of regression outputs from the GWR model for buildup land and population change during 1970–1990.

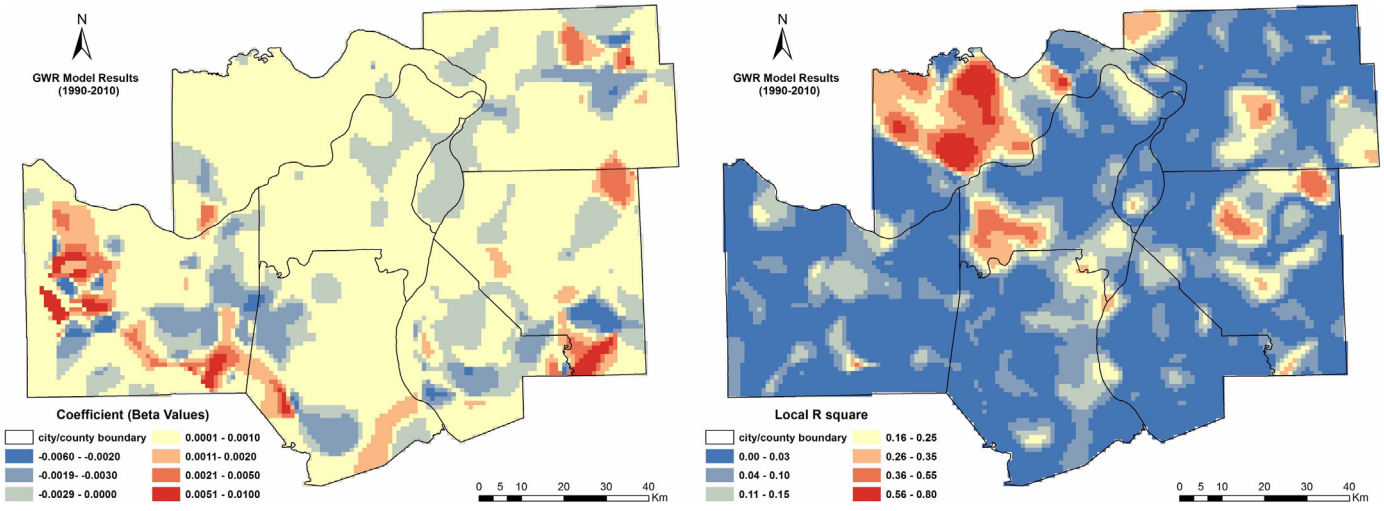

Fig. 13. Spatial variation of regression outputs from the GWR model for buildup land and population change during 1990–2010.

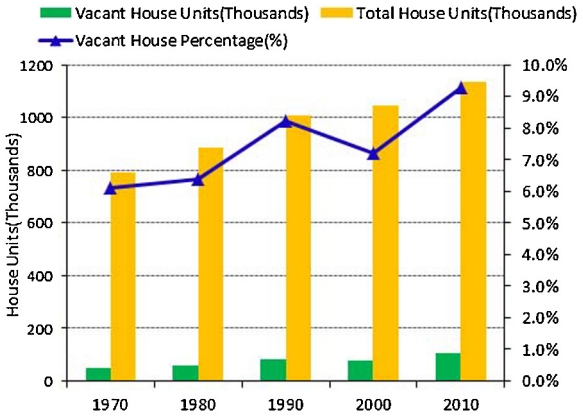

Fig. 14. Vacant and total house units and vacant house percentage of study area from 1970 to 2010.

and negative correlations were revealed by the GWR model. Relatively strong positive relationships and higher R^2 were located in outer suburbs. As expected, the relationships in urban core, specifically over the northwest part of St. Louis city and east part of St. Louis County, were significant with higher R^2. During 1990–2010, both significant positive and negative correlations (Fig. 13) were found comparing to the results from Pearson's correlation coefficient (Table 5) and OLS model (Table 8). Fig. 13 illustrated that significant positive relationships with higher R^2 were located in St. Charles County, southwest of St. Louis County, and south part of St. Louis City.

Discussion

Multiple studies have focused on the relationship between urban growth, LCLUC, and socioeconomic data, but few applied both global and local level statistics to reveal detailed spatial and temporal characteristics of shrinking cities (Huang et al., 2011; Ma et al., 2008; Romero et al., 2012). As one of the shrinking cities in the US (Hackworth, 2014), this St. Louis study will provide insights for the causes of declining of the post-industrial US cities. In this paper, we integrated remote sensing and census data based on grid cells using both global level (OLS) and local level (GWR) statistical methods, which offered a richer framework for understanding detailed spatial and temporal patterns and trends of urban growth (Bagan and Yamagata, 2012; Banzhaf et al., 2013; Martinuzzi et al., 2007).

Urban growth in the STL region presents a strong feature of decentralization in central city and inner suburbs. The growth has spread to outer suburbs over the past 40 years (Figs. 5 and 8). The rate of buildup land growth was 58.99%, which exceeded the rate of population growth (9.74%) by a factor of 6.1 (percent of buildup change/percent of population change). This spread was likely due to the social preference for low-density housing, suburban lifestyle, and well-developed highway systems. This outcome could also be associated with high crime rates and failing urban schools in the core areas of the STL region. In addition, urban growth in STL lead to continues growth of vacant houses, especially in urban core and inner suburban areas (Figs. 14–16). The spatial distribution of population during this period (Figs. 9 and 10) also indicated a certain degree of racial and environmental segregation.

Urban growth patterns in STL are different from that of China and India (Bhatta, 2009; Deng et al., 2008), where the cities are experiencing fast urbanization, and the population tends to increase in the urban core. This pattern is also different than some cities in developed countries, such as Tokyo, which has been experiencing suburbanization and sprawl but without serious

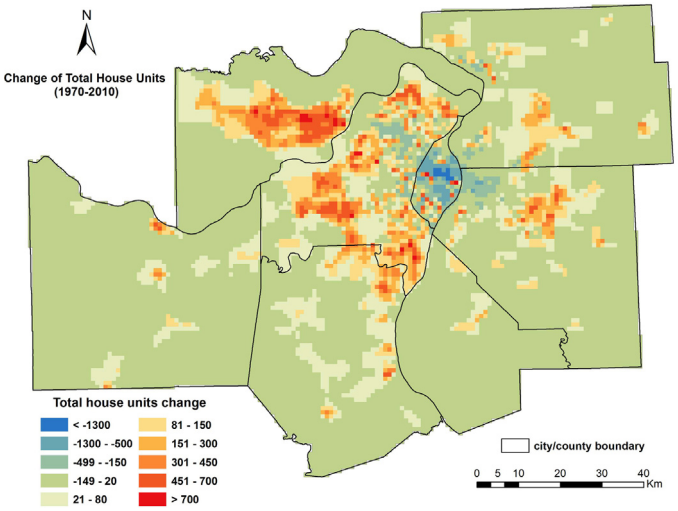

Fig. 15. Change of total house units spatially from 1972 to 2010.

shrinking in urban core and social segregation (Bagan and Yamagata, 2012).

With the growth of the population in outer suburbs in STL, the amount of field land, such as cropland and grassland, has been converted to buildup land. However, in the core urban areas, buildup land slightly increased or decreased within the St. Louis city limits depending on the different time intervals, which was partly owing to the neighborhood revitalization programs in the study area and/or land clearance policy (Gordon, 2008). This result was also confirmed by the change of total and vacant house units in this area (Figs. 15 and 16). Field land has continuously decreased with the urban expansion since 1970. However, a slight increase was found in urban core, which was partly due to governmental land clearance policy. High negative correlation between forest and field lands were found (Tables 5 and 6), which might be attributed to the fact that much of the reforestation is occurring on former agricultural land. It is worth noting that market forces and the work of local community organizations that desire more trees due to their esthetic appeal were also one of the causes of increased forest land (Manson and Evans, 2007). Water was relatively stable and it counted for about 2.5% of the land in the STL region, but water increased to 3.9% in 2010 probably due to the increased precipitation

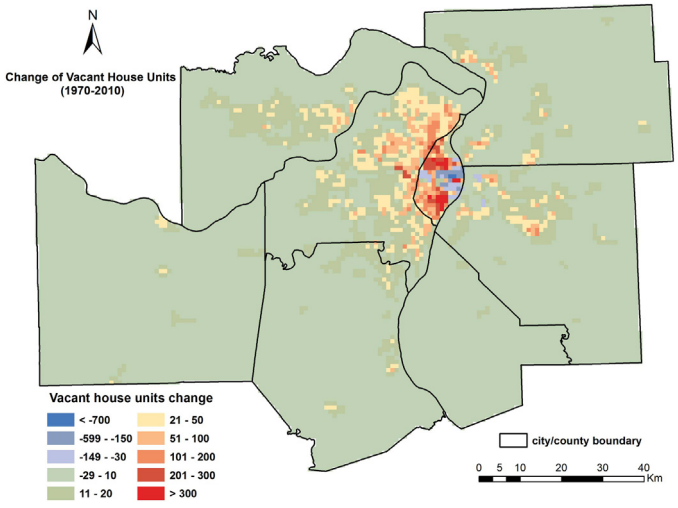

Fig. 16. Change of vacant house units spatially from 1972 to 2010.

during the image capture. Observation records from the National Weather Service Weather Forecast Office showed that monthly river stages and precipitation in 2010 was much higher than that in other years (NOAA, 2014).

Buildup land changes were positively correlated with population changes during 1970–2010 time interval. However, these relationships were not consistent over time. For example, the correlation was negative during 1970–1990 and positive during 1990–2010. This was partly due to the rapid decrease of total population during 1970–1982 and increase since 1980 (Fig. 7) with a continued increase of buildup land in STL region.

The spatial analysis based on grid cells has great advantages as demonstrated by this paper. However, one notable limitation of this method is the Modifiable Areal Unit Problem (MAUP) associated with scale and zoning effects. The scale of the grid cell and the gridding methods would affect the results (Lo and Yang, 2002; Openshaw and Taylor, 1979; Su et al., 2012). In addition, we converted census tract population data to gird cells and calculated population in each grid and then correlated the grid cell data with LCLUC grid data. However, census designated tracts are often determined arbitrarily and represent aggregated population, and therefore, do not take into account the spatial configuration of the population within the census tract area (Holt et al., 2004). This may have generated overestimates of the population in the unpopulated and sparsely populated areas, and underestimated the population density in more-densely populated areas. Dasymetric maps which consider build environments and spatial configuration of population within census tract could reduce this error to some extent (Kimerling et al., 2009), which is the future study of this paper. Moreover, urban growth is associated with a number of physical factors including LCLU change, landscape change, proximity of urban center to residential areas, highways, shopping centers, and neighborhood socioeconomic factors (e.g., population, income, poverty and employment densities changes etc.) (Lo and Yang, 2002; Sanford and Maryville, 2011). We mainly considered LCLU and population change as characteristics of urban growth, which is another limitation of this paper.

Conclusions

Based on remote sensing derived land use changes and socioeconomic factors, this study provided spatial and temporal dynamics of urban growth in the St. Louis metropolitan region over the last 40 years. The STL region has experienced rapid urban expansion especially along the outer suburbs at the cost of cropland and grassland, while such changes were accompanied by massive population decentralization and migration in urban core resulting in growing vacancy and intense racial and environmental segregation in traditional city.

A grid-cell-based spatial relationship using OLS and GWR models showed that urban sprawl was overall positively correlated with population change during 1970–2010 at the global level. However, this relationship was not linear over time, and was negative during the 1970–1990 time-period and positive during the 1990–2010 time-period. Spatial heterogeneity and variations in the relationship revealed that urban sprawl was positively correlated with population changes in outer suburbs and negatively correlated in central city and inner suburbs. Spatiotemporal analysis using global and local level statistics allowed us to demonstrate the process of urban growth and its causal association with population change.

The paper demonstrated a robust framework that integrates disparate spatial and temporal data from many different sources (i.e., remote sensing, census, field measurements, etc.) into a single comprehensive dataset to conduct spatial analysis to support decision making and sustainable planning.

Acknowledgements

The first author would like to express his gratitude to the China Scholarship Council (CSC) for their important scholarship for visiting scholars. “Current Vegetation 2010” data were provided by the Missouri Resource Assessment Partnership (MoRAP) and East-West Gateway Council of Governments. We would like to thank anonymous reviewers for their constructive comments.

References

Akaike, H., 1974. A new look at the statistical model identification. IEEE Trans. Autom. Control 19, 716–723.
Alperovich, G., Deutsch, J., 1992. Population-density gradients and urbanization measurement. Urban Stud. 29, 1323–1328.
Anderson, J.R., 1976. A land use and land cover classification system for use with remote sensor data. US Government Printing Office.
Arnfield, A.J., 2003. Two decades of urban climate research: a review of turbulence, exchanges of energy and water, and the urban heat island. Int. J. Climatol. 23, 1–26.
Bagan, H., Yamagata, Y., 2012. Landsat analysis of urban growth: how Tokyo became the world's largest megacity during the last 40 years. Remote Sens. Environ. 127, 210–222.
Banzhaf, E., Reyes-Paecke, S., Muller, A., Kindler, A., 2013. Do demographic and land use changes contrast urban and suburban dynamics? A sophisticated reflection on Santiago de Chile. Habitat Int. 39, 179–191.
Bellehumeur, C., Legendre, P., 1998. Multiscale sources of variation in ecological variables: modeling spatial dispersion, elaborating sampling designs. Landsc. Ecol. 13, 15–25.
Berry, B.J.L., 1990. Urbanism, colonialism, and the world-economy – cultural and spatial foundations of the world urban system. J. Asian Stud. 49, 617–619.
Bhatta, B., 2009. Analysis of urban growth pattern using remote sensing and GIS: a case study of Kolkata, India. Int. J. Remote Sens. 30, 4733–4746.
Bhatta, B., Saraswati, S., Bandyopadhyay, D., 2010. Quantifying the degree-of-freedom, degree- of-sprawl, and degree-of-goodness of urban growth from remote sensing data. Appl. Geogr. 30, 96–111.
Cohen, W.B., Goward, S.N., 2004. Landsat's role in ecological applications of remote sensing. Bioscience 54, 535–545.
Cortes, C., Vapnik, V., 1995. Support-vector networks. Mach. Learn. 20, 273–297.
De Freitas, M.W.D., dos Santos, J.R., Alves, D.S., 2013. Land use and land cover change processes in the Upper Uruguay Basin: linking environmental and socioeconomic variables. Landsc. Ecol. 28, 311–327.
Deng, X., Huang, J., Rozelle, S., Uchida, E., 2008. Growth, population and industrialization, and urban land expansion of China. J. Urban Econ. 63, 96–115.
Foody, G.M., Mathur, A., 2006. The use of small training sets containing mixed pixels for accurate hard image classification: training on mixed spectral responses for classification by a SVM. Remote Sens. Environ. 103, 179–189.
Fortin, M.J., 1999. Effects of sampling unit resolution on the estimation of spatial autocorrelation. Ecoscience 6, 636–641.
Fortin, M.J., Dale, M.R.T., 2009. Spatial autocorrelation in ecological studies: a legacy of solutions and myths. Geogr. Anal. 41, 392–397.
Fortin, M.J., Payette, S., 2002. How to test the significance of the relation between spatially autocorrelated data at the landscape scale: a case study using fire and forest maps. Ecoscience 9, 213–218.
Fotheringham, A.S., Brunsdon, C., Charlton, M., 2003. Geographically Weighted Regression: The Analysis of Spatially Varying Relationships. John Wiley & Sons.
Fox, J., 2003. People and the Environment: Approaches for Linking Household and Community Surveys to Remote Sensing and GIS. Springer.
Frumkin, H., 2002. Urban sprawl and public health. Public Health Rep. 117, 201–217.
Gallego, F.J., 2010. A population density grid of the European Union. Popul. Environ. 31, 460–473.
Gillies, R.R., Box, J.B., Symanzik, J., Rodemaker, E.J., 2003. Effects of urbanization on the aquatic fauna of the Line Creek watershed, Atlanta – a satellite perspective. Remote Sens. Environ. 86, 411–422.
Gordon, C.E., 2008. Mapping Decline: St. Louis and the Fate of the American City. University of Pennsylvania Press.
Griffiths, P., Hostert, P., Gruebner, O., van der Linden, S., 2010. Mapping megacity growth with multi-sensor data. Remote Sens. Environ. 114, 426–439.
Hackworth, J., 2014. The limits to market-based strategies for addressing land abandonment in shrinking American cities. Progr. Plan. 90, 1–37.
Hamilton, L.C., Press, D., 1992. Regression with Graphics: A Second Course in Applied Statistics. Duxbury Press, Belmont.
Han, D., Chan, L., Zhu, N., 2007. Flood forecasting using support vector machines. J. Hydroinf. 9, 267–276.
Harries, K., 2006. Extreme spatial variations in crime density in Baltimore County, MD. Geoforum 37, 404–416.
Hasse, J.E., Lathrop, R.G., 2003. Land resource impact indicators of urban sprawl. Appl. Geogr. 23, 159–175.
Herold, M., Goldstein, N.C., Clarke, K.C., 2003. The spatiotemporal form of urban growth: measurement, analysis and modeling. Remote Sens. Environ. 86, 286–302.
Holt, J.B., Lo, C., Hodler, T.W., 2004. Dasymetric estimation of population density and areal interpolation of census data. Cartogr. Geogr. Inf. Sci. 31, 103–121.

Huang, C., Davis, L.S., Townshend, J.R.G., 2002. An assessment of support vector machines for land cover classification. Int. J. Remote Sens. 23, 725–749.
Huang, S.C., Wang, H.W., 2006. Combining time-scale feature extractions with SVMs for stock index forecasting. Neural Inf. Process. 4234 (Pt 3), 390–399.
Huang, G., Zhou, W., Cadenasso, M.L., 2011. Is everyone hot in the city? Spatial pattern of land surface temperatures, land cover and neighborhood socioeconomic characteristics in Baltimore, MD. J. Environ. Manag. 92, 1753–1759.
Jat, M.K., Garg, P.K., Khare, D., 2008. Monitoring and modelling of urban sprawl using remote sensing and GIS techniques. Int. J. Appl. Earth Obs. 10, 26–43.
Jensen, J.R., 2009. Remote Sensing of the Environment: An Earth Resource Perspective 2/e. Pearson Education India.
Jordan, Y.C., Ghulam, A., Hartling, S., 2014. Traits of surface water pollution under climate and land use changes: a remote sensing and hydrological modeling approach. Earth-Sci. Rev. 128, 181–195.
Jordan, Y.C., Ghulam, A., Herrmann, R.B., 2012. Floodplain ecosystem response to climate variability and Land cover and Land use change in Lower Missouri River basin. Landsc. Ecol. 27, 843–857.
Kalnay, E., Cai, M., 2003. Impact of urbanization and land use change on climate. Nature 423, 528–531.
Kelly, M., Estes, J.E., Knight, K.A., 1999. Image interpretation keys for validation of global land cover data sets. Photogramm. Eng. Remote Sens. 65, 1041–1050.
Kimerling, A.J., Buckley, A.R., Muehrcke, P.C., Muehrcke, J.O., 2009. Map Use: Reading and Analysis. Esri Press.
Kolios, S., Stylios, C.D., 2013. Identification of land cover/land use changes in the greater area of the Preveza peninsula in Greece using Landsat satellite data. Appl. Geogr. 40, 150–160.
Lambin, E.F., Geist, H.J., Lepers, E., 2003. Dynamics of land use and land cover change in tropical regions. Annu. Rev. Environ. Resour. 28, 205–241.
Lo, C.P., Yang, X.J., 2002. Drivers of land use and land cover changes and dynamic modeling for the Atlanta, Georgia Metropolitan Area. Photogramm. Eng. Remote Sens. 68, 1073–1082.
Lopez, T.D., Aide, T.M., Thomlinson, J.R., 2001. Urban expansion and the loss of prime agricultural lands in Puerto Rico. Ambio 30, 49–54.
Lu, D.S., Weng, Q.H., 2006. Use of impervious surface in urban land use classification. Remote Sens. Environ. 102, 146–160.
Ma, M., Lu, Z., Sun, Y., 2008. Population growth, urban sprawl and landscape integrity of Beijing city. Int. J. Sust. Dev. World 15, 326–330.
Manson, S.M., Evans, T., 2007. Agent-based modeling of deforestation in southern Yucatán, Mexico, and reforestation in the Midwest United States. Proc. Natl. Acad. Sci. U. S. A. 104, 20678–20683.
Mantero, P., Moser, G., Serpico, S.B., 2005. Partially supervised classification of remote sensing images through SVM-based probability density estimation. IEEE Trans. Geosci. Remote 43, 559–570.
Martin, D., 1996. Geographic Information Systems: Socioeconomic Applications. Psychology Press.
Martinuzzi, S., Gould, W.A., Gonzalez, O.M.R., 2007. Land development, land use, and urban sprawl in Puerto Rico integrating remote sensing and population census data. Landsc. Urban Plan. 79, 288–297.
Moran, P.A., 1950. Notes on continuous stochastic phenomena. Biometrika 37, 17–23.
MRLC, 2008. Multi-resolution Land Characteristics Consortium (MRLC) (2008). National Land Cover Database (NLCD) 1992/2001 retrofit land cover change product, Available at: http://www.mrlc.gov/nlcdrlc.php
NOAA, 2014. National Oceanic and Atmospheric Administration (NOAA) (2014). National Climatic Data Center, Available at: http://www.ncdc.noaa.gov/
NWS, 2014. National Weather Service archives – St. Louis Office, Available at: http://www.crh.noaa.gov/lsx/?n=cli_archive
Openshaw, S., Taylor, P.J., 1979. A million or so correlation coefficients: three experiments on the modifiable areal unit problem. In: Wrigley, N. (Ed.), Statistical Applications in the Spatial Sciences, vol. 21, pp. 127–144.
Poelmans, L., Van Rompaey, A., 2009. Detecting and modelling spatial patterns of urban sprawl in highly fragmented areas: a case study in the Flanders-Brussels region. Landsc. Urban Plan. 93, 10–19.
Radeloff, V.C., Hagen, A.E., Voss, P.R., Field, D.R., Mladenoff, D.J., 2000. Exploring the spatial relationship between census and land cover data. Soc. Nat. Resour. 13, 599–609.
Romero, H., Vásquez, A., Fuentes, C., Salgado, M., Schmidt, A., Banzhaf, E., 2012. Assessing urban environmental segregation (UES). The case of Santiago de Chile. Ecol. Ind. 23, 76–87.
Ryznar, R.M., Wagner, T.W., 2001. Using remotely sensed imagery to detect urban change: viewing Detroit from space. J. Am. Plann. Assoc. 67, 327–336.
Sanford, S.W., Maryville, M., 2011. A Technique for Mapping Urban Areas and Change Using Integrated Remote Sensing and Dasymetric Population Mapping Methods.
Sexton, J.O., Urban, D.L., Donohue, M.J., Song, C.H., 2013. Long-term land cover dynamics by multi-temporal classification across the Landsat-5 record. Remote Sens. Environ. 128, 246–258.
Small, C., Elvidge, C.D., Balk, D., Montgomery, M., 2011. Spatial scaling of stable night lights. Remote Sens. Environ. 115, 269–280.
Sokal, R.R., 1974. Classification: purposes, principles, progress, prospects. Science 185, 1115–1123.
Song, C., Woodcock, C.E., Seto, K.C., Lenney, M.P., Macomber, S.A., 2001. Classification and change detection using Landsat TM data: when and how to correct atmospheric effects? Remote Sens. Environ. 75, 230–244.
Squires, G.D., Friedman, S., Saidat, C.E., 2002. Experiencing residential segregation – a contemporary study of Washington, DC. Urban Aff. rev. 38, 155–183.
Su, S.L., Xiao, R., Zhang, Y., 2012. Multi-scale analysis of spatially varying relationships between agricultural landscape patterns and urbanization using geographically weighted regression. Appl. Geogr. 32, 360–375.
Sutton, P.C., 2003. A scale-adjusted measure of "Urban sprawl" using nighttime satellite imagery. Remote Sens. Environ. 86, 353–369.
Tu, J., 2013. Spatial variations in the relationships between land use and water quality across an urbanization gradient in the watersheds of Northern Georgia, USA. Environ. Manag. 51, 1–17.
Tu, J., Xia, Z.G., 2008. Examining spatially varying relationships between land use and water quality using geographically weighted regression. I: model design and evaluation. Sci. Total Environ. 407, 358–378.
United Nations, Department of Economic and Social Affairs, Population Division, 2014. World Urbanization Prospects: The 2014 Revision.
Verburg, P.H., Eickhout, B., van Meijl, H., 2008. A multi-scale, multi-model approach for analyzing the future dynamics of European land use. Ann. Reg. Sci. 42, 57–77.
Xian, G., Crane, M., 2005. Assessments of urban growth in the Tampa Bay watershed using remote sensing data. Remote Sens. Environ. 97, 203–215.
Xian, G., Crane, M., 2006. An analysis of urban thermal characteristics and associated land cover in Tampa Bay and Las Vegas using Landsat satellite data. Remote Sens. Environ. 104, 147–156.
Xiao, J.Y., Shen, Y.J., Ge, J.F., Tateishi, R., Tang, C.Y., Liang, Y.Q., Huang, Z.Y., 2006. Evaluating urban expansion and land use change in Shijiazhuang, China, by using GIS and remote sensing. Landsc. Urban Plan. 75, 69–80.
Yang, L.M., Xian, G., Klaver, J.M., Deal, B., 2003. Urban land cover change detection through sub-pixel imperviousness mapping using remotely sensed data. Photogramm. Eng. Remote Sens. 69, 1003–1010.
Yuan, F., Sawaya, K.E., Loeffelholz, B.C., Bauer, M.E., 2005. Land cover classification and change analysis of the twin cities (Minnesota) Metropolitan area by multitemporal Landsat remote sensing. Remote Sens. Environ. 98, 317–328.
Zhang, L.J., Gove, J.H., 2005. Spatial assessment of model errors from four regression techniques. For. Sci. 51, 334–346.